

Optimising the FDM additive manufacturing process to achieve maximum tensile strength: A state of the art review.

T.Gordelier^{a,*}, P.R.Thies^a, L.Johanning^a, L.Turner^b

^a*Renewable Energy Research Group, University of Exeter, Penryn Campus, Cornwall, UK, TR10 9FE.*

^b*3D Kernow, Concept Shed, Falmouth, UK, TR11 3EX.*

Abstract

Additive manufacturing or ‘3D printing’ is a rapidly expanding sector and is moving from a prototyping service to a manufacturing service in its own right. With a significant increase in sales, Fused Deposition Modelling (FDM) printers are now the most prevalent 3D printer on the market. The increase in commercial manufacturing necessitates an improved understanding of how to optimise the FDM printing process for various product mechanical properties.

This paper seeks to identify optimum print parameters for the FDM process to achieve maximum tensile strength through a review of recent studies in this field. The effect of the governing printing parameters on the tensile strength of printed samples will be considered, including: material selection, print orientation, raster angle, air gap and layer height.

Key findings include material recommendations, such as the use of emerging print materials like polyether-ether-ketone (PEEK) to produce samples with tensile strength over 200% that of conventional materials such as acrylonitrile butadiene styrene (ABS). Amongst other parameters it is shown that printing in the ‘upright’ orientation should be avoided (samples can be up to 50% weaker in this orientation) and air gap and raster width should be concurrently optimised to ensure good ‘inter-raster’ bonding. The optimal choice of raster angle depends on print material; in ABS for example, selecting a 0° raster angle over a 90° angle can increase tensile strength by up to 100%.

The paper conclusions provide researchers and practitioners with an up to date, single point reference, highlighting a series of robust recommendations to optimise the tensile strength of FDM printed samples. Improving the mechanical performance of FDM printed samples will support the continued growth of this technology as a viable production technique.

Keywords: FDM, tensile strength, raster angle, ABS, PLA, print orientation, air gap.

*Corresponding author

Email address: T.J.Gordelier@exeter.ac.uk (T.Gordelier)

1. Introduction

Additive manufacturing (AM) is a rapidly expanding sector and is anticipated to continue growing as detailed in Figure 1 [1]. The advantages it represents over conventional manufacturing technologies have led to a rapid up-take across many sectors. This cross sector applicability is also clearly demonstrated in Figure 1.

Historically AM technology was utilised for prototype production, but increasingly it is being seen as a production technique in its own right [2]. A 2017 global review of over 900 AM users found that whilst 34% and 23% of respondents use AM for prototype and proof of concept development respectively, a surprising 22% already use it for production purposes [3]. This increase in production printing has led to great interest in the material properties of AM products, with manufacturers keen to demonstrate to their customers that their products can meet certain standards. Despite the apparent need, to date, no specific material property tests are available for AM products as will be discussed in Section 3. To add to this uncertainty, many different printing technologies are available and within each technology group there are numerous printing parameters and material options available for any given printer. This leads to a large variation in the physical properties of AM products.

The range of printing technologies available is detailed in Figure 2 and demonstrates that, in 2017, Fused Deposition Modelling (FDM) is the most common technique. This study also finds that plastics are the most common printing material, utilised by 88% of respondents. Given this is the most common printing technique, it will form the focus of the paper here and the FDM printing process will be briefly summarised in Section 2.

Many studies have been conducted to consider the impact of printing parameters on the quality of the end product for FDM printing. To date, no one paper is available that summarises this large body of work, and sets out key printing parameters to optimise component strength. This paper therefore seeks to amalgamate these studies and provide a useful reference for anyone hoping to optimise the FDM printing process to achieve maximum tensile strength of their printed components. Additive manufacturing is a rapidly developing technology and as such, this paper focuses on recent studies from 2014 onwards. Where a

Abbreviations: ABS: Acrylonitrile butadiene styrene AM: Additive manufacturing DE: Differential evolution CAD: Computer aided design COV: Coefficients of variation FDM: Fused deposition modelling FE: Finite element FEA: Finite element analysis FLM: Fused layer modelling GMDH: Group method of data handling MIA: Multi-layered iteration PEEK: Polyether-ether-ketone PC: Polycarbonate PLA: Polylactic acid RepRap: Replicating rapid prototyper SEM: Scanning electron microscope SLA: Stereolithography STL file: Stereolithography file - often used to export CAD files in preparation for AM printing TPE: Thermoplastic elastomer UTS: Ultimate tensile strength XRD: X-ray powder diffraction

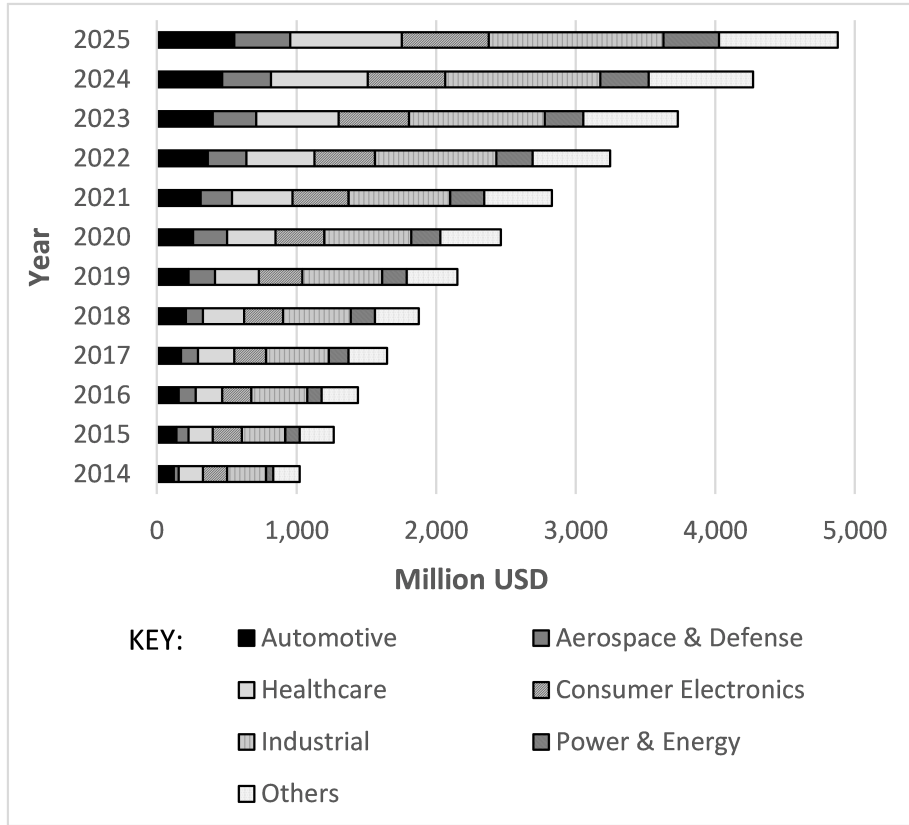


Figure 1: U.S. 3D printing market forecast by year, 2014-2025. Summarised from [1].

study is felt to be particularly relevant however, some earlier findings will be included.

Within this paper, firstly, the adopted test methods will be reviewed in Section 3, the results will then be highlighted in Section 4, and reasons for the observed variation in strength will be covered in the Discussion, Section 5. Finally, Conclusions in Section 6 will summarise the optimal FDM printing parameters to maximise component tensile strength.

2. The FDM process

Before detailing the FDM process, it should be noted that this process is also referred to as Fused Filament Fabrication (FFF). The term FDM was trademarked by Stratysys Inc. and hence an alternative name, FFF, was developed by some users to avoid conflict. The two names refer to identical technology.

As outlined in Section 1, FDM printing is one of the most widely adopted forms of AM and many publications outline the printing process in detail; a

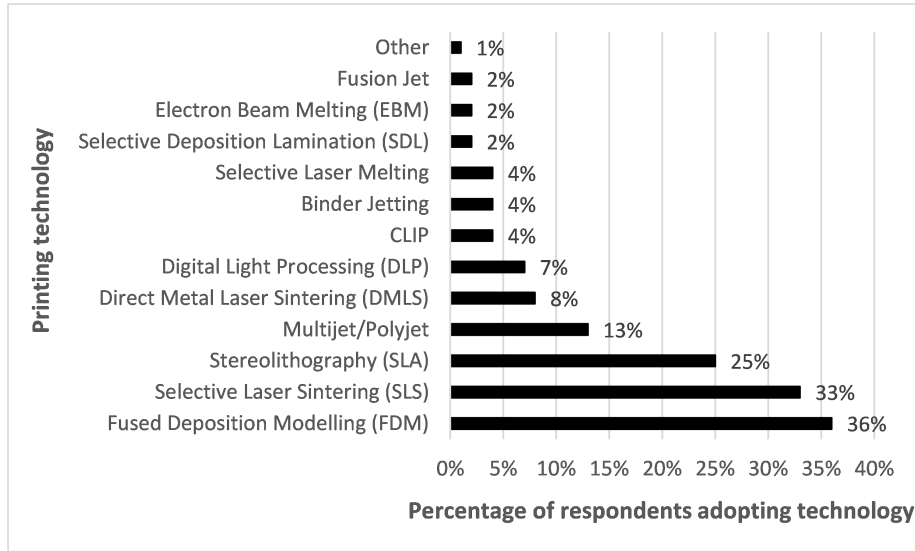


Figure 2: 3D printing technologies adopted by respondents, from a 2017 global survey of 900+ users. Summarised from [3].

selection of these are included for reference [4, 5, 6, 7]. A detailed explanation of the physical phenomena behind the FDM printing process is also provided by [8]. In this section, a brief summary of the process will be provided with reference to Figure 3 which outlines the key components of a FDM printer. The first step of printing a FDM component is to develop a computer aided design (CAD) model of the component. The CAD model is commonly exported as a stereolithography (STL) file which is then ‘sliced’ by specialist 3D printing software and read by the printer to print the component in a series of ‘sliced’ layers. A spool of printing filament is drawn through the extruder head, which heats the filament to a semi-molten state. It is then forced through an extrusion nozzle and onto the printer build platform. The extruder head (or the build platform) is able to move around in the X-Y plane creating a 2D slice of the required part. Once the first layer is complete, the extruder head (or the build platform) will move in the Z direction, to enable a second layer of 2D material to be applied on-top of the first. The semi-molten state of the material allows adjacent layers to fuse together forming the 3D solid layer by layer. Some 3D structures may have overhangs, and as such require a support structure during the printing process. For this there are two main options: The FDM printer can print the support structure (or ‘scaffolding’) in a more fragile state so that it can be clipped off once printing is complete. Alternatively, some printers use a second nozzle utilising a different material to print the support structure concurrently with the main component. The support structure is then removed once printing is complete (often the support structure material is soluble for example).

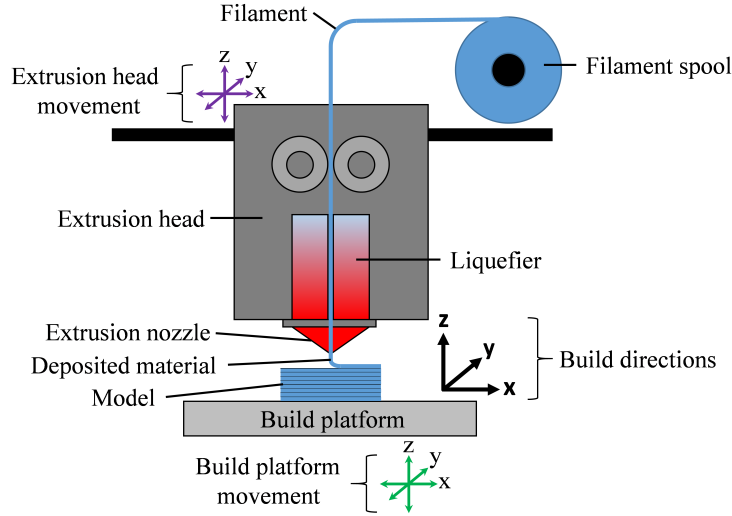


Figure 3: Key components of a FDM printer. Movement is achieved in the x, y and z direction by either movement of the extrusion head (purple arrows), movement of the build platform (green arrows) or a combination of the two e.g. x and y direction achieved by movement of the extrusion head and z direction achieved by movement of the build platform. Developed from original image by [6].

A further progression of the commercial FDM printer came through the development of the ‘RepRap Printer’, short for replicating rapid prototyper. This printer, based on FDM technology, is essentially self-replicating and a ‘parent’ printer can print out a significant proportion of the parts required to build a ‘child’ printer, with the remaining parts being widely and cheaply available. The ‘RepRap’ project started in 2004, with the first ‘child’ machine manufactured at Bath University in 2008 [9]. The design of the printer is open source and free to access, with many variants available; this has led to very low production costs and correspondingly large global uptake. The high prevalence of these printers further adds to interest on how to optimise the printing process, and some of the studies considered later in this paper will look at optimising the tensile strength of ‘RepRap’ printed components.

With the basics of FDM printer technology explained, the next section sets out the different methodologies applied by the sector to test FDM printed products for tensile strength.

3. Applied methodologies

To date, no specific guidance is available to quantify the tensile strength of AM products, and most studies have referred to existing tensile strength tests for materials such as polymers or composite materials. It was anticipated that a recent publication from DNV GL, ‘DNVGL-CF-0197 Additive manufacturing

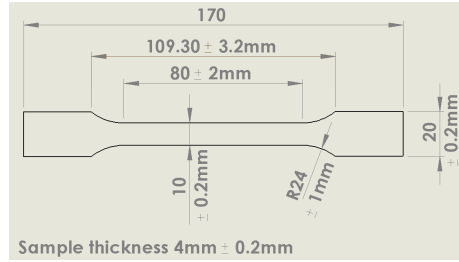


Figure 4: Dimensions for specimen 1A of ISO 527-2-1996 standard for the determination of tensile properties of moulding and extrusion plastics [12].

- *qualification and certification process for materials and components*’ [10], may help to bridge this lack of guidance, however this publication refers to generic paths for qualification and cites a range of existing test methodologies rather than specifically creating a new standard for AM.

Despite this lack of guidance, many studies have investigated the effect of numerous printing parameters on the final printed product. Within these studies a range of methodologies have been adopted to quantify the tensile strength of printed samples. The approaches fall into one of two categories: The ‘Hourglass’ type specimen, utilising a dumbbell or hourglass shaped test piece and covered in Section 3.1, and the alternative ‘Rectangular’ type specimen, utilising a rectangular shaped test piece and covered in Section 3.3. The following sections will review the two broad approaches adopted by the majority of studies discussed here and highlight potential weaknesses with these approaches.

3.1. ‘Hourglass’ tensile test methodology

There are two key test standards that have been widely adopted by the sector utilising the ‘hourglass’ type tensile test specimen, these are the ASTM D638 *Standard test method for tensile properties of plastics* [11] and the equivalent ISO standard, BS EN ISO 527-2-1996 *Plastics. Determination of tensile properties. Part 2: Test conditions for moulding and extrusion plastics* [12]. The ISO 527 standard has 5 parts, with part 1 focusing on the general testing principles and the remaining 4 parts identifying testing methodologies for a range of different plastics. Part 2 represents an ‘hourglass’ type specimen as detailed in Figure 4 and is the most widely adopted methodology of the ISO 527 standard in the AM work reviewed. The ASTM D638 standard is more flexible in terms of sample geometry than the more prescriptive ISO 527-2, with a range of test specimens to choose from. However, both standards adopt broadly similar sample dimensions.

As this paper is focused on the FDM printing approach, those studies looking to investigate FDM printed samples will be highlighted. Of these studies the ASTM D638 approach is adopted by [13, 14, 4, 15, 16, 17, 18, 19, 20] and [6]. Indeed a review paper by [21] demonstrates this is a popular approach for reviewing the tensile strength of products from a range of rapid prototyping techniques, not just FDM. The alternative, but similar ISO 527-2 approach is

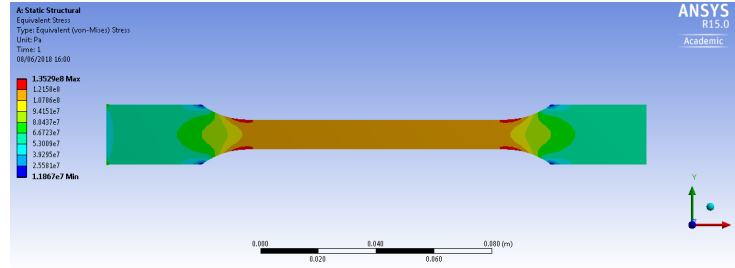


Figure 5: FEA model demonstrating the equivalent stress in an ISO 527-2 specimen 1A (dimensions as detailed in Figure 4). Model is subject to a tensile load of 5,000N. The peak stress in red occurs adjacent to the bend radii.

adopted by [22, 23, 24, 25, 26] and [27]. The ISO 527-3 approach [28] (specifically for films and sheets) also utilises an ‘hourglass’ shaped sample and is utilised by [27].

There are three further studies that have adopted an ‘hourglass’ type tensile test specimen, though have not specifically followed either the ASTM D628 or the ISO 527-2 test methodology. These are [23, 29] and [30].

Although the majority of these studies report valid results when adopting the above approach some issues with this type of methodology have been reported by [7] and others, and will be highlighted below.

3.2. Issues with ‘hourglass’ methodology

The principal of the ‘hourglass’ specimen is that the failure occurs in the gauge length of the sample where the sample is thinnest. However it has been noted in some studies that premature failures of some samples have occurred at the bend radius, outside of the gauge length of the specimen. A simple finite element analysis (FEA) demonstrates that the geometry of the sample leads to stress concentrations at these points, as detailed in Figure 5.

The issue of early sample failures is investigated by [31] who originally intended to follow the ASTM D638 standard to characterise the properties of FDM printed ABS. On preliminary testing the samples were found to fail prematurely on the bend radius due to these stress concentrations. This study highlights that the issue is compounded by the FDM manufacturing process where the radii is approximated by the termination of raster lengths as highlighted in Figure 6.

This issue is also raised by [17], who in earlier work had adopted the ASTM D638 methodology [13]. However, during an investigation into the effects of layer parameters on the tensile strength of FDM printed ABS [17] also observe premature sample failures on the radii of the samples. This research identifies a particular issue for thin specimens printed in certain orientations. To obtain reliable results across the range of samples under investigation this study reverted to rectangular shaped geometry, nominally based around the sample dimensions of the ASTM D638 ‘hourglass’ shape.

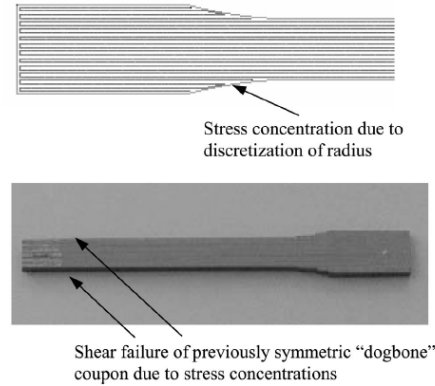


Figure 6: Tensile tests conducted by [31] demonstrate issues with premature shear failure at the sample radius due to stress concentrations developing. Image replicated from [31].

Further to these studies [14] also uses the ASTM D638 approach for a comparative study of ABS and PLA specimens printed using a ‘RepRap’ type printer. This study states that “*many specimens broke outside of the gauge length due to assumed stress concentrations in the regions changing geometry*”. Despite observing this during the experimental phase, the data from these investigations were reported as valid results.

It is of concern that further studies utilising the discussed methodologies do not interpret an issue with the obtained results if the samples fail outside of the gauge length. Only a limited number of studies publish images of failed specimens which makes it challenging to establish the validity of results. Helpfully, a study by [25] utilising the ISO 527-2 approach to characterise properties of FDM printed ABS samples publish an image demonstrating a selection of failed specimens, this is replicated in Figure 7. Of the 15 specimens detailed only three demonstrate fracture within the gauge length of the samples, with the remaining failures occurring at, or very near, the radii. Again, it appears in this study that all these samples were included as valid results.

A single example image of a failed specimen is published by [27] who utilise an ‘hourglass’ specimen to review a range of materials from both FDM and SLA printing. This image also demonstrates a failure at the radius of the samples but no reference is made to this being a rejected sample or out of scope.

For both of these examples, these out of range failures could be considered a ‘worst-case-scenario,’ underestimating the true strength of the material. Inclusion of these results in the reported data should therefore not lead to over optimistic conclusions and can perhaps be justified on this basis. However, it is surprising to see no discussion of this in the presented reports.

Some studies include details of samples that have successfully broken within the sample gauge length including [15, 29, 18] and [6]. It is a valuable contribution that all the publications discussed above do provide details on the failed samples, whether deemed ‘successful’ or not. Many of the studies however, do

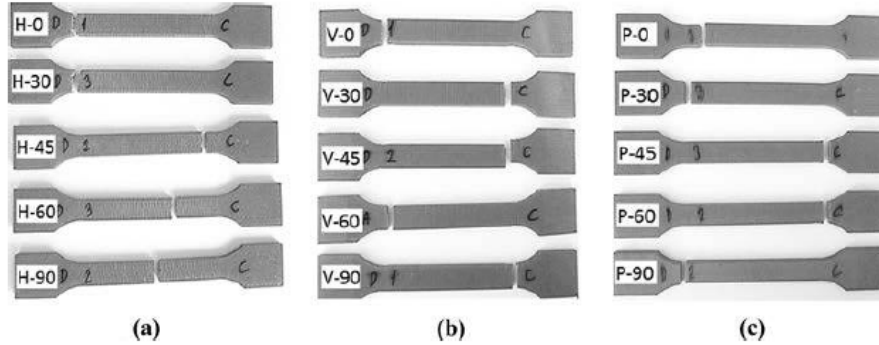


Figure 7: Results published in [25] highlighting the range of failure modes when utilising ISO 527-2 to investigate the characteristics of FDM printed ABS. The samples were printed with a range of raster angles at the following orientations: (a) Horizontal orientation. (b) Vertical orientation. (c) Perpendicular orientation. All samples excluding row (a) H-60, H-90 and H-45 demonstrate failure at the sample radius. Image replicated from [25].

not publish this information which raises concerns regarding whether early failures occurred at the sample radii and if so, how this could affect the validity of the results.

Given these concerns regarding the ‘hourglass’ type specimens, alternative methodologies are discussed below.

3.3. Alternative methodologies

The main issue with the ‘hourglass’ shaped specimen is the stress concentration around the radii due to the sample geometry. This issue is intensified by the FDM technique which essentially lays the material in lines (often referred to as ‘roads’ or ‘rasters’) resulting in manufacturing discontinuities at these radius points. It is therefore helpful to refer to testing standards for other materials that have similar anisotropy in their formation, such as fibre reinforced composites. Some studies have looked to these standards for guidance.

The equivalent standards are (i) BS EN ISO 527-5:2009 *Plastics. Determination of tensile properties. Part 5: Test conditions for uni-directional fibre-reinforced plastic composites* [32] and correspondingly (ii) ASTM D3039-17 *Standard test method for tensile properties of polymer matrix composite materials* [33]. Both these standards adopt rectangular shaped specimens and therefore avoid the issues created by the radii of the ‘hourglass’ specimens.

There are however, far fewer examples of these standards being adopted in the literature. The ASTM D3039 standard is utilised by [31] when comparing the tensile strength of FDM manufactured ABS parts directly to injection moulded parts. It is also adopted by [34] and [5] to investigate the effect of various printing parameters on the tensile strength of FDM printed ABS. Composite testing experts Intertek suggest utilising the ASTM D3039 standard instead of

the ‘hourglass’ ASTM D638 standard for AM applications suggesting it is “recommended for highly oriented and/or high modulus fibre reinforced polymer composites” [35].

There is limited adoption of the ISO 527-5 standard, although it is referred to by [36] who propose a methodology for single layer AM specimens and state that this standard is applicable due to “structural analogies” between AM specimens and fibre-reinforced plastics.

Having considered the various approaches adopted by the sector for quantifying the tensile strength of samples, the next section will detail the results obtained across the various studies.

4. Tensile strength optimisation results

4.1. Material selection

A range of materials can be utilised with FDM printing, and new materials are continually being added to the available selection. Two of the most common materials utilised at the time of writing are ABS and PLA. [26] utilise the ISO 527 approach adopting the specimen dimensions in Figure 4 to investigate the comparative strength of these two samples and conclude that PLA demonstrates 1.2 to 1.5 times the yield strength of ABS. This study also considers the specific strength of the specimens, which takes into account the density of the specimen in addition to the strength. Again, PLA demonstrates the strongest response with a specific strength 1.1 to 1.3 times that of ABS.

The ‘RepRap’ printer technology introduced in Section 2 is utilised by [14] who also investigate the relative merits of PLA and ABS, this time utilising the ASTM D638 standard. Across the range of variables tested PLA is shown to have twice the tensile strength of ABS. The study also discusses the relative strength of these parts in comparison to commercial 3-D printers and concludes they can produce parts of comparable strength. However, in comparison to injection moulded specimens, the study concludes that although PLA can achieve similar strength, ABS parts are generally weaker than the injection moulded alternatives.

ABS is compared to another material, polycarbonate (PC), by [6] using the ASTM D638 methodology. Across all printing parameters investigated PC samples demonstrates significantly higher tensile strength at break than the ABS samples. The strongest PC sample was manufactured with an ‘on-edge’ print orientation (described further in Section 4.3) and a $\pm 45^\circ$ raster angle. The tensile strength of this sample at break was 1.9 times that of the equivalent ABS sample.

A comparatively newer material to the market polyether-ether-ketone (PEEK) is compared to ABS by [29] utilising small 75mm long ‘hourglass’ tensile test specimens. This study concludes that the tensile strength of PEEK samples is on average 108% higher than ABS. The study also suggests that further improvements could be made to the mechanical strength of PEEK samples through further optimisation of the printing techniques adopted for this newer material.

In addition to alternative materials, some studies have considered the use of additives with standard materials to develop composites in order to improve mechanical properties. A detailed review of FDM fibre reinforced polymers is provided by [8] who summarise numerous studies that investigate the potential advantages of these composite materials. This review concludes that continuous fibre reinforced composites are significantly stronger than discontinuous fibre composites, achieving strength comparable to aluminium in some instances. The direction of loading also plays a significant role, with loading perpendicular to the raster beads resulting in much weaker components. The concept of anisotropy in FDM printed parts will be further explored in Sections 4.2 and 4.3.

One such example of a composite study is conducted by [15] who compare standard ABS to ABS with 5 wt.% discontinuous jute fibre (Cyclolac®, GE ABS resin), ABS with 5 wt.% titanium dioxide (TiO₂) and an ABS polymeric blend with 5 wt.% of a thermoplastic elastomer (TPE). Utilising the ASTM D638 standard the tensile strength of each variant is investigated and only the ABS with TiO₂ is shown to improve the tensile strength of the standard ABS samples, increasing the UTS by 13.2% on average. The jute composite and the TPE blend actually reduce the UTS by 9% and 16% respectively. This work is continued in a further study, [37], which focuses on ABS polymer matrix composites and polymer blends. Although this study demonstrates that some of these additives can lead to a reduction in sample anisotropy, this comes at the expense of UTS with a reduction in overall sample tensile strength. For further studies relating to FDM fibre reinforced composites see [8].

Even within each material classification there are variations between the specific feedstock utilised for printing and [38] consider the tensile strength of specimens printed from a range of different coloured PLA filaments (white, blue, grey, black and natural). Utilising the ASTM D638 standard, this study demonstrates that natural PLA (with no added dye) has the highest tensile strength whilst grey PLA has the lowest. On average, the samples printed with natural PLA have an ultimate tensile strength 12% higher and a yield strength 14% higher than the grey samples. Blue, white and black PLA samples have tensile strengths scattered between these two extremes.

To summarise the large number of studies considering the effect of material selection on component strength, Table 1 has been included.

In addition to material selection, numerous printing parameters can be varied to optimise the printing process and the following sections will review these.

4.2. Raster orientation

The most common printing variable to be investigated to optimise FDM printing is the raster angle. Raster angle denotes the angle at which the rasters, or roads, are laid during the construction of each layer during the FDM process as detailed in Figure 8. Many printers default to a $\pm 45^\circ$ angle however this variable can usually be controlled to either print at one angle or at an alternating angle for each layer. A total of 13 studies have been identified that have

Table 1: Summary of studies investigating the effect of material selection on printed sample tensile strength. Table notes: *Denotes studies utilising ‘RepRap’ printer technology

Author(s)	Variables considered	Material for max tensile strength	Notes
Ebel et al. 2014 [26]	ABS and PLA	PLA	PLA 1.2 to 1.5 times stronger than ABS.
Tymrak et al. 2014 [14]*	ABS and PLA	PLA	PLA twice the tensile strength of ABS averaged across all sample variations.
Cantrell et al. 2017 [6]	ABS and PC	PC	PC 1.9 times strength of ABS.
Wu et al. 2015 [29]	ABS and PEEK	PEEK	PEEK 108% stronger than ABS.
Torrado Perez et al. 2014 [15]	ABS, ABS with jute, ABS with TiO2, ABS with TPE	ABS with TiO2	TiO2 increased strength by 13.2%. All other additives reduced the tensile strength.
Wittdrodt et al. 2015 [38]*	PLA filament colour (natural, white, blue, black and grey)	Natural (12% higher UTS than grey)	Related to having the lowest crystallinity.
Breken et al. 2018 [8]	Review of fibre reinforced polymers	Nylon with 18% carbon fibre	Continuous fibre composites strongest.

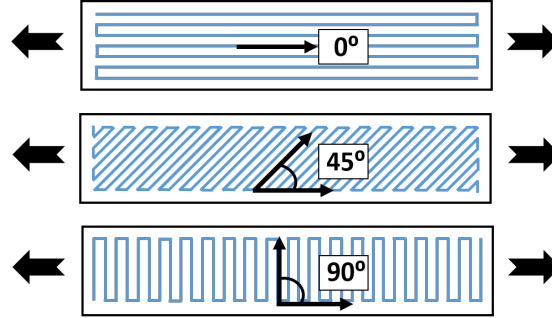


Figure 8: Raster angle definition. Blue lines identify raster pattern and large black arrows identify direction of tensile loading. In this paper, raster angle will be defined from 0° being fully aligned with the tensile loading direction to 90° being perpendicular to the tensile loading direction.

295 considered the raster orientation and will be detailed below in sub-sections relating to printing material. Conventional printing practice generally utilises a solid outer skin filled with an internal structure to speed up printing time and minimise material use. This is specified by the pattern of the structure and a % infill value, with machines often defaulting to 20% infill. However, for the
 300 experimental investigations reported below, unless otherwise stated, the samples are printed at 100% infill i.e. solid blocks. Although this is not normally adopted in general printing practice, this ensures that it is the material and printing parameters that are investigated as opposed to the print construction.

4.2.1. Raster angle for ABS

305 Four raster angles are considered by [31]: 0° , $\pm 45^\circ$, $0^\circ/90^\circ$ and 90° utilising the ASTM D3039 approach. This study concludes that the 0° angle (where the tensile strength is carried along the direction of the raster) has the highest tensile strength, approaching twice the strength of samples printed with a 90° angle. The specimens printed with $\pm 45^\circ$ and $0^\circ/90^\circ$ raster angle demonstrate
 310 similar tensile strength, higher than the 90° specimens and lower than the 0° specimens.

A complex statistical approach is utilised by [22] to investigate the effect of numerous printing parameters on the material properties of ABS samples utilising ISO 527-2 specimens. Three raster angles are investigated, 0° , 30° and
 315 60° . The paper does not provide a definition of the terminology used so it is assumed that the angles are specified in accordance with the majority of other studies i.e. as in Figure 8. Although many variables are considered, the samples with the highest UTS are printed with a raster angle of 60° . Reasons for this finding will be addressed in the Discussion, Section 5.2.

320 A similar study is conducted by [34] who use ASTM D3039 to consider raster angles of 0° , 45° , 90° and $\pm 45^\circ$ in FDM ABS samples and also compare these to the tensile strength of injection moulded parts. Here, the highest tensile strength is achieved with a 0° raster angle followed by $\pm 45^\circ$ (which failed at

75% the strength of the 0° samples). On average, the 0° specimens obtain
325 a tensile strength of 94.8% compared to an injection moulded equivalent. The
study also considers the tension-tension fatigue performance of the samples with
 $\pm 45^\circ$ demonstrating the highest cycles to failure.

The work by [25] utilises ISO 527-2 to investigate the effect of five different
raster angles (0° , 30° , 45° , 60° , 90°) on a range of mechanical properties. This
330 study also considers the effect of print orientation on these mechanical properties
which will be explained in Section 4.3. For standard printing orientations (flat or
'on-edge') the 0° raster angle demonstrates the highest tensile strength. For the
upright print orientation (which would not usually be adopted in conventional
printing practice) the 90° raster angle demonstrates the highest tensile strength.

A further study by [39] utilises a multi-layered iterative (MIA) group method
of data handling (GMDH) algorithm to investigate optimal parameters for FDM
printing applying differential evolution (DE). Experimental results applying the
ISO 527-2 process are utilised to verify the mathematical model. Pre-tests are
conducted to inform the algorithm and the full suite of tests consider two raster
340 angles 0° and 90° . The developed algorithm then calculates the optimal process
parameters for tensile strength. Many different variables are investigated and
although raster angle is shown not to be the most significant factor influencing
tensile strength, the optimal raster angle for tensile strength is found to be 50° .

A finite element (FE) model of FDM specimens is developed by [16] who
345 compare FE results to physical testing following the ASTM D638 test procedure.
Three raster angles are considered 0° , 45° and 90° . Although summary data
of results is not provided in the paper, graphical results of the physical tests
clearly demonstrate the maximum UTS is obtained with a raster angle of 0° .

Further investigations are conducted by [5] who utilise the rectangular ASTM
350 D3039 specimens to investigate the strength of a range of raster angles and layer
thickness on the tensile strength of FDM printed ABS. Three raster angles are
considered, 0° , 45° and 90° and across the range of variables considered samples
printed with a 0° raster angle demonstrated the highest tensile strength.

An investigation by [19] utilises slightly different terminology, but also con-
355 sider the effect of raster angle on the strength of specimens printed to the
ASTM D638 standard. Within this standard a range of specimen sizes are
considered and this investigations reviews the results from 'hourglass' Type I,
IV and V specimens. In this work 'longitudinal' refers to a raster angle of 0° ,
'cross-hatched' refers to a raster angle alternating by 90° between subsequent
360 print layers i.e. $0^\circ/90^\circ$, and 'transversal' refers to a raster angle of 90° relative
to the length of the specimen. For the two larger specimens investigated, Type
I and IV, a raster angle of 0° produced samples with the highest UTS, however
for the smaller sample Type V, a raster angle of $0^\circ/90^\circ$ produced the highest
UTS.

365 Raster angle, build direction and material are investigated by [6] who compare
both ABS and PC using ASTM D638. Two different raster angles are
considered for the ABS samples: $\pm 45^\circ$ and $0^\circ/90^\circ$. This study finds very little
difference between the UTS of the samples with different raster angles. A raster
angle of $0^\circ/90^\circ$ resulted in a UTS 3.7% and 3.0% higher than the $\pm 45^\circ$ for

370 samples printed in a flat and upright orientation respectively. In the on-edge
printing orientation $0^\circ/90^\circ$ samples were 2.3% weaker. These small differences
between sample strengths are insignificant, particularly when considering con-
fidence intervals of the data.

The final study to be discussed here by [14] was introduced in Section 4.1 and
375 utilises a ‘RepRap’ type printer to investigate the effect of raster angle on ABS
utilising the ASTM D638 standard. Two raster angles are considered: $0^\circ/90^\circ$
and $\pm 45^\circ$. The results demonstrate very little variation in tensile strength
between the two types of sample investigated, although the strongest samples
were printed with a $0^\circ/90^\circ$ raster angle.

380 Due to the large number of studies discussed here, a summary of the results
regarding selection of raster angle when printing in ABS is detailed in Table 2.

This section has summarised the results from investigations looking at ABS
and the next two sections will summarise findings from alternative materials.

4.2.2. Raster angle for PLA

385 Fewer studies have looked into the effect of raster angle on the tensile
strength of PLA specimens. [13] investigate the effect of 3 different raster angles
utilising ASTM D638. Raster angles of 0° , 90° and 45° are investigated and
a raster angle of 45° is found to produce the strongest specimens, on average
10% stronger than the 0° printed specimens. The study also considers fatigue
390 performance of the specimens and concludes 45° and 0° have the best fatigue
performance, with 45° performing better at lower stress levels and 0° performing
better at higher stress levels.

A further study is conducted by [18] who also consider both tensile strength
and fatigue performance. This study utilises different terminology, considering
395 printing along the X-direction, the Y-direction and at an angle of 45° . Given the
print head for the particular printer technology utilised always moves parallel
to the X-direction, the print direction of the printed part can be considered
a proxy for variation in the raster angle; 0° , 90° and 45° respectively. This
study finds that those samples utilising a raster angle of 0° are nearly 25%
400 stronger than those printed at an angle of 90° , with samples printed at an angle
of 45° achieving UTS values between these two. Fatigue testing demonstrates
a different order of success, with optimum fatigue performance achieved by
samples with a 45° raster followed by 90° and finally 0° raster angles.

A very different testing approach is adopted by [30] who, instead of printing
405 specimens to particular dimensions, print 100% solid blocks of PLA and sub-
sequently machine the test samples from these blocks. ‘Hour-glass’ tensile test
specimens are machined, but they are not manufactured to meet a particular
tensile test standard in this instance. Three different raster angles are used in
the printing of the original blocks, 0° , 90° and 45° . These FDM printed PLA
410 samples are also compared to conventional injection moulded samples. Two
different strain rates are investigated in this study and at both strain rates, the
samples with rasters at 45° achieve the highest UTS. The largest difference was
achieved at the higher strain rate, where the 45° specimens were 32.8% stronger
than the 90° specimens which were the weakest. In contrast to expectations, at

Table 2: Summary of studies investigating the effect of raster angle on ABS printed sample tensile strength. Table notes: [†]Many of these studies consider multiple variables and as such there is not one raster angle that achieves maximum tensile strength across all variables; the angle reported here results in maximum tensile strength for the majority of variables investigated. *Denotes studies utilising ‘RepRap’ printer technology.

Author(s)	Raster angles investigated	Raster angle for max tensile strength [†]	Notes
Ahn et al. 2002 [31]	0°, ±45°, 0°/90°, 90°	0°	0° approx 2 times stronger than 90°
Sood et al. 2010 [22]	0°, 30°, 60°	60°	Many other variables investigated
Ziemian et al. 2012 [34]	0°, 45°, 90°, ±45°	0°	Second strongest ±45° at 75% strength of 0°
Durgan et al. 2014 [25]	0°, 30°, 45°, 60°, 90°	0°	0° best when printing flat or ‘on-edge’ only
Rayegani et al. 2014 [39]	0°, 45°	50°	50° calculated by applying a DE algorithm to test data
Rezayat et al. 2015 [16]	0°, 45°, 90°	0°	Full numerical data not provided
Rankouhi et al. 2016 [5]	0°, 45°, 90°	0°	Many variables investigated
Torrado et al. 2016 [19]	0°, 0°/90°, 90°	0°	0° optimal for larger specimens I and IV. 0°/90° optimal for smaller specimen V.
Cantrell et al. 2017 [6]	±45°, 0°/90°	n/a	No significant difference observed.
Tymrak et al. 2014 [14]*	0°/90°, ±45°	0°/90°	0°/90° showed a small advantage over ±45°

Table 3: Summary of studies investigating the effect of raster angle on PLA printed sample tensile strength. Table notes: [†]Some of these studies consider multiple variables and as such there is not one raster angle that achieves maximum tensile strength across all variables; the angle reported here results in maximum tensile strength for the majority of variables investigated. *Denotes studies utilising ‘RepRap’ printer technology.

Author(s)	Raster angles investigated	Raster angle for max tensile strength [†]	Notes
Letcher et al. 2014 [13]	0°, 90°, 45°	45°	45° on average 10% stronger than 0°.
Afrose et al. 2016 [18]	0°, 90°, 45°	0°	0° approx 25% stronger than 90°.
Song et al. 2017 [30]	0°, 90°, 45°,	45°	Printed in blocks, then shaped.
Tymrak et al. 2014 [14]*	0°/90°, ±45°	0°/90°	Not a large improvement but 0°/90° marginally stronger.

the higher strain rate, the 45° and 0° specimens were 24.2% and 11.0% stronger than the injection moulded specimens respectively. At the lower strain rate investigated, all three raster angle directions produced samples with strength exceeding the UTS of the injection moulded samples.

Finally, the study introduced in Section 4.1 by [14] also investigated the relative strength of PLA samples printed using a ‘RepRap’ printer. Again, two angles were studied: 0°/90° and ±45°. Minimal variation in tensile strength was observed between these two defined raster angles, though the highest samples were achieved with a 0°/90° raster angle.

A summary of the investigations and results for raster angle selection in PLA is detailed in Table 3.

4.2.3. Alternative materials

The majority of the published literature regarding FDM printing focuses on the common materials utilised in industry: ABS and PLA. An additional material is investigated in a study by [4] who consider samples printed in polycarbonate (PC) utilising the ASTM D638 standard. This study uses a different notation to previous studies addressed and unlike Figure 8 the angles are defined where 90° is a sample with rasters aligned along the length of the loading path. For clarity in reporting, these results will be converted to the same notation as the other studies considered. This study gradually alters the raster angle in 15° increments, and clearly demonstrates that the closer the raster angle is to

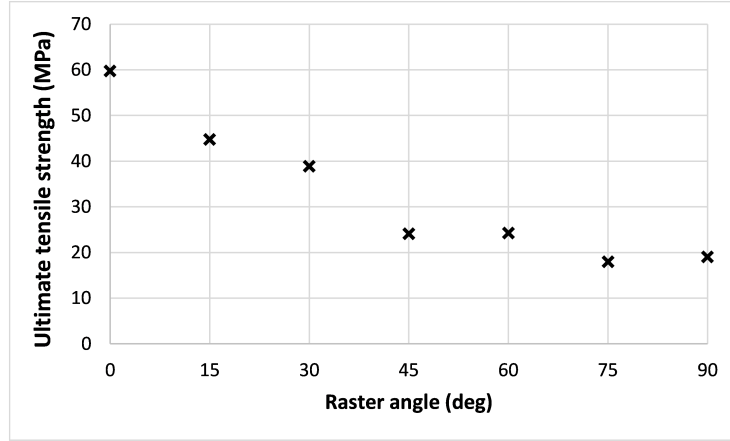


Figure 9: Variation in ultimate tensile strength with print raster angle for polycarbonate (PC) samples tested to the ASTM D638 standard. Average UTS of 6 specimens for each raster angle detailed. These results are replicated from [4] and revised to align with the raster nomenclature adopted in this paper. UTS has been converted from PSI to MPa.

alignment with the direction of the tensile load applied, the higher the UTS. For samples with fully aligned raster angles (0° in the other studies we have considered) the UTS is approximately 3 times the strength of samples where the load is applied perpendicular to the raster (90°). Figure 9 details the average results from this study, revised to reflect the angle notation adopted in this review paper.

PC is further considered in a study by [6] which was introduced in Section 4.2.1. Four different raster angles are considered which differ from those investigated in other studies: $\pm 45^\circ$, $+30^\circ / -60^\circ$, $+15^\circ / -75^\circ$ and $0^\circ / 90^\circ$. The study also investigates the effect of print orientation, which affects the optimal raster orientation selected. For samples printed flat on the printer bed (as detailed in Figure 10) raster angles of $\pm 45^\circ$ and $+15^\circ / -75^\circ$ have similar tensile strength properties and produce significantly stronger samples than the other angles investigated. For the other print orientations, on-edge and upright, only two raster angles are investigated, $\pm 45^\circ$ and $0^\circ / 90^\circ$. Very little difference is observed between the two raster angles, with a raster angle of $\pm 45^\circ$ producing samples with very marginally higher UTS.

Further to this [29] consider the effect of raster angle on the tensile strength of PEEK samples considering $0^\circ / 90^\circ$, $30^\circ / -60^\circ$ and $\pm 45^\circ$. The $0^\circ / 90^\circ$ samples were significantly stronger than the other samples, demonstrating tensile strength 35.4% and 30.7% higher than $30^\circ / -60^\circ$ and $\pm 45^\circ$ respectively.

A summary of the investigations and results for raster angle selection in alternative materials is detailed in Table 4.

Having considered the effect of raster angle on the tensile strength of FDM printed materials, the next section will consider the effect of print orientation.

Table 4: Summary of studies investigating the effect of raster angle on polycarbonate (PC) and polyether-ether-ketone (PEEK) printed sample tensile strength. Table notes: [†]Some of these studies consider multiple variables and as such there is not one raster angle that achieves maximum tensile strength across all variables; the angle reported here results in maximum tensile strength for the majority of variables investigated.

Author(s)	Material and raster angles investigated	Raster angle for max tensile strength [†]	Notes
Hill et al. 2014 [4]	PC: 0° - 90° in 15° increments	0°	0° is 3 times stronger than 90°.
Cantrell et al. 2017 [6]	PC: ±45°, 0°/90°, +30°/-60°, +15°/-75°	±45° and +15°/-75°	Optimal results for flat orientation samples only.
Wu et al. 2015 [29]	PEEK: 0°/90°, ±45° 30°/-60°,	0°/90°	0°/90° is 35.4% stronger than 30°/-60°.

4.3. Print orientation

When printing a component, the choice of printing orientation relative to the printer build platform can be selected so that the sample is printed flat, on-edge, or upright. A good diagram is produced by [20] which clearly describes these print orientations, and is replicated in Figure 10. The choice of build orientation can affect the mechanical properties of the samples, and this is investigated by the studies reported below.

For ABS samples print orientation is investigated by [25], who consider flat printing, on-edge printing and upright printing as identified in Figure 10 (the terminology used in this particular paper are horizontal, vertical and perpendicular respectively). Across a range of raster angles investigated, this study concludes that flat and on-edge printing produce significantly stronger samples than upright, typically achieving strengths 50% - 100% higher than samples printed in the upright direction. There is minimal variation in strength between the flat and on-edge printed specimens; on the whole the flat specimens were stronger, although the individual sample maximum strength was achieved with an on-edge print and a 0° raster angle. Reasons for this variation in strength will be discussed in Section 5.3.

A similar study is repeated by [6] who also consider the same three print directions across a range of raster angles for both ABS and PC samples. Considering the ABS samples, very little variation in UTS is observed between any of the orientations investigated.

The PC samples investigated by [6] show much more sensitivity to printing orientation, with those printed on-edge showing the highest tensile strength, closely followed by the flat print orientation. The upright printed samples are

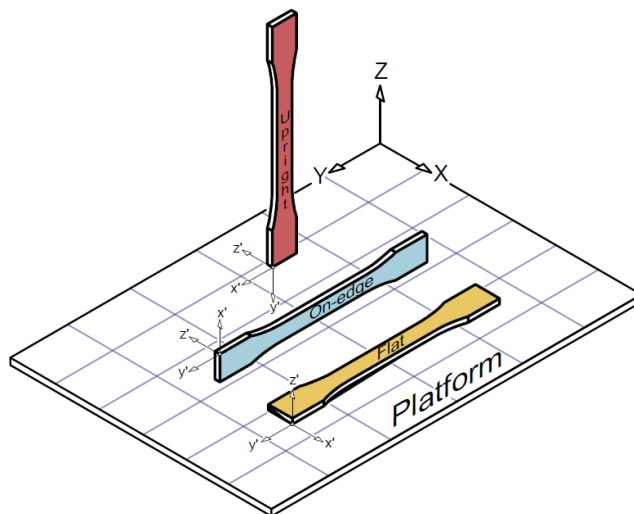


Figure 10: The different build orientation options available for FDM printed samples as published by [20].

significantly weaker. The strongest sample printed in PC is achieved with an on-edge printing direction and a raster angle of $\pm 45^\circ$; this shows an average UTS 29.8% stronger than an upright specimen with $\pm 45^\circ$ raster angle.

Finally, printing direction is considered for PLA samples by [20] who also consider the three printing orientations described above in addition to varying layer thickness. This study finds that flat and on-edge printed samples have comparable tensile strength performance, with both being significantly stronger than upright samples. In many cases these samples exhibit twice the UTS of upright printed samples.

A summary of the studies and results investigating the effect of print orientation across a range of materials is detailed in Table 5.

4.4. Layer height

Layer height is a further printing parameter that can be selected during the printing process and it controls the height of each printed layer. Although not as thoroughly investigated as the previous topics, the following studies investigate the impact of layer height on the tensile strength of FDM printed samples.

The multi-variate study conducted by [22] into FDM printed ABS samples considers the effect of printing layer height on sample tensile strength. Three layer heights are considered: 0.127mm, 0.178mm and 0.254mm. The findings are not explicit in the report, however, the response surfaces published in this paper appear to show the highest UTS is achieved utilising the thickest layer height across the range of variables investigated. Potential reasons for this behaviour are discussed in Section 5.4.

The effect of layer height on ABS parts is further considered by [5] who consider two layers heights, 0.2mm and 0.4mm. This study also varies the total

Table 5: Summary of studies investigating the effect of print orientation on printed sample tensile strength of ABS, PC and PLA. Table notes: [†]Some of these studies consider multiple variables and as such the print orientation reported here results in maximum tensile strength for the majority of variables investigated.

Author(s)	Material and print orientation investigated	Print orientation for max tensile strength [†]	Notes
Durgun et al. 2014 [25]	ABS: Flat, on-edge, upright	Flat and on edge	Minimal diff' between flat and on edge. Typically 50-100% stronger than up-right.
Cantrell et al. 2017 [6]	ABS: Flat, on-edge, upright	None	Minimal diff' observed between any orientations.
Cantrell et al. 2017 [6]	PC: Flat, on-edge, upright	On-edge	Flat also performed well but upright much weaker.
Chacon et al. 2017 [20]	PLA: Flat, on-edge, upright	Flat and on-edge	Minimal diff' between flat and on-edge. Often twice the strength of upright.

thickness of the samples tested from 0.2mm to 7mm. Across the full range of sample thicknesses investigated, 0.2mm printed layers consistently result in higher sample UTS. This appears to contradict the findings presented above by [22] and reasons for this will be addressed in the Discussion section 5.4.

515 As previously discussed [14] utilise ‘RepRap’ type printers to investigate the tensile strength of both ABS and PLA printed samples. This study also considered the effect of varying three layer heights: 0.4mm, 0.3mm and 0.2mm. For the ABS samples, layer height made minimal difference; samples printed with the lowest height, 0.2mm, demonstrated marginally higher UTS. In the PLA
520 samples however, layer height made a more significant difference; on average samples adopting a 0.2mm layer height had 24.5% and 10.0% greater UTS than samples printed with a 0.3mm and 0.4mm layer height respectively.

The effect of layer height on the UTS of PLA samples is also investigated by [20] who consider 4 layer heights: 0.06mm, 0.12mm, 0.18mm, 0.24mm. This
525 study also investigates print orientation (as discussed in Section 4.3) and filament feed rate (which will be discussed in Section 4.6). In the upright build orientation, which has significantly lower UTS than on-edge or flat build orientations, a larger layer height increases the UTS across all feed rates investigated. For the on-edge and flat print directions, an increase in layer height has limited
530 effect on UTS at the lowest feed rate (20mm/s) but at the higher feed rates (50mm/s and 80mm/s) an increase in layer height is observed to reduce the UTS. The strongest samples were printed in the flat orientation with the thinnest layer height, 0.06mm. Reasons for these observed behaviours will be further discussed in Section 5.4.

535 Given the number of studies investigating the effect of layer height on tensile strength, a summary of the results is detailed in Table 6.

4.5. Air gap and raster width

Some printing parameters can have a similar effect on the printed specimens and this is certainly true of air gap and raster width. During printing the defined
540 air gap is the space left between the rasters (or roads) of deposited material, and the raster width is the specified width of the deposited raster, as detailed in Figure 11. These two variables can be optimised together to ensure overlap or a gap between adjacent rasters.

The air gap between rasters is considered by [16] who also investigate the effect of a range of variables on the tensile strength of ABS samples. Three
545 air gaps are considered in this work -0.05mm, 0.0mm and 0.05mm. Across the range of raster angles investigated, increasing the air gap consistently reduces the UTS of the sample, with an air gap of -0.05mm always achieving the highest strength for any given raster angle. A change in air gap has a more significant
550 impact on samples printed with a raster angle of 45° and 90° than it does to samples with a raster angle of 0°. This will be discussed in Section 5.5. The maximum sample UTS is obtained with an air gap of -0.05mm and a raster angle of 0°.

A study by [39] considers the effect of both air gap and raster width on
555 ABS printed samples. Two different air gaps are considered, -0.00254mm and

Table 6: Summary of studies investigating the effect of layer height on printed sample tensile strength of ABS and PLA. Table notes: [†]Some of these studies consider multiple variables and as such the layer height reported here results in maximum tensile strength for the majority of variables investigated. *Represents studies utilising ‘RepRap’ printer technology.

Author(s)	Layer thicknesses investigated	Layer thickness for max tensile strength [†]	Notes
Sood et al. 2010 [22]	ABS: 0.127mm, 0.178mm, 0.254mm	Variable - not clear	Paper suggests thinner layers can initially add strength but also increase sample distortion.
Rankouhi et al. 2016 [5]	ABS: 0.2mm, 0.4mm	0.2mm	0.2mm layer is strongest across all raster angles considered.
Tymrak et al. 2014 [14]*	PLA: 0.4mm, 0.3mm, 0.2mm	0.2mm	0.2mm layer is significantly stronger.
Tymrak et al. 2014 [14]*	ABS: 0.4mm, 0.3mm, 0.2mm	0.2mm	0.2mm layer is only marginally stronger.
Chacon et al. 2017 [20]	PLA: 0.06mm, 0.12mm, 0.18mm, 0.24mm	0.06mm	Variable results depending on print direction and feed rate. Strongest samples use 0.06mm.

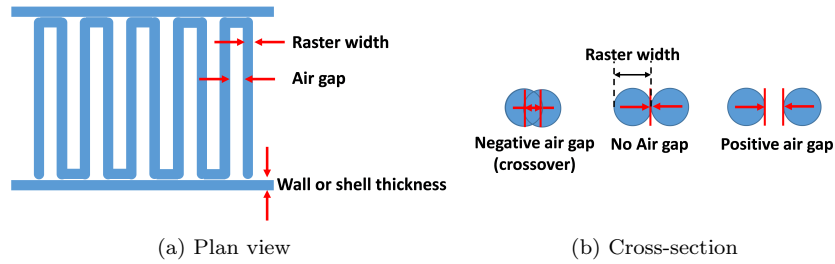


Figure 11: Air gap and raster width definitions for FDM printing. (a) Details a plan view of the raster pattern showing a positive air gap between adjacent rasters. (b) Details the effect of air gap selection on the cross-section through adjacent deposited rasters.

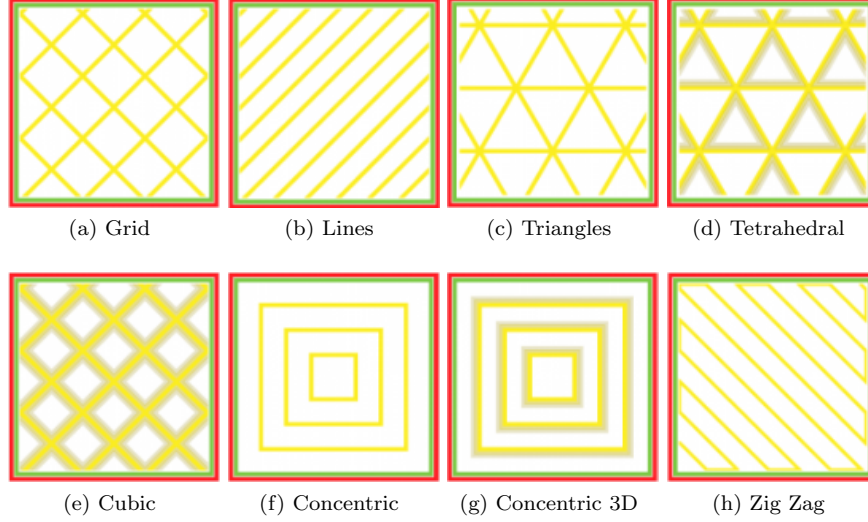


Figure 12: Range of infill options available with Ultimaker replicated from [40].

0.5588mm, and two different raster widths, 0.2034mm and 0.5588mm. Other variables are also considered in this study but consistently the negative air gap resulted in a higher sample UTS for all combinations of the other variables. For a negative air gap, an increase in raster width slightly reduces the UTS of the samples across the range of variables tested. Conversely, for a positive air gap a higher raster width increases the relative UTS of the samples, although it should be noted that overall the samples are much weaker than the samples with a negative air gap. Reasons for this will be addressed in Section 5.5.

4.6. Other variables

There are numerous printing variables that can be altered during FDM printing, and those investigated most commonly have been discussed in the sections above. There are some variables that have not been widely investigated but can still have an effect on the tensile strength of printed samples and these will be detailed below.

Although the majority of studies addressed above have adopted a 100% infill for the printed samples, in practice, many practitioners will save money, time and materials by printing the outline of a shape and infilling it at a reduced infill density. In addition to specifying the infill density, there are numerous infill patterns available and this will clearly effect the strength of a sample. Figure 12 outlines the various infill options with a leading printer manufacturer, Ultimaker [40].

A full investigation of the pros and cons of all these options has not been conducted but a study by [26] investigates the yield strength and specific strength of both ABS and PLA when printed to either a 100% infill structure, utilising a

580 45° raster angle, or a honeycomb infill structure made from multiple hexagonal prisms. The infill density selected for the honeycomb structure is unfortunately not specified in the paper, although printers commonly default to 20% infill. This study also investigates a range of different printer outputs; here those samples printed on a Felix 1.0e will be discussed for consistency. For samples
585 printed in ABS the 100% infill samples had over twice the yield strength of the honeycomb structure, and the PLA samples had around 2.5 times the yield strength. This is not a surprising result but the values for specific strength (σ_S), calculated by Equation 1 are perhaps more informative. Here σ_T = tensile strength and ρ = material density.

$$\text{Specific strength, } \sigma_S = \left(\frac{\sigma_T}{\rho} \right) \quad (1)$$

590 In ABS, the specific strength of the 100% infill samples were approximately 1.4 times the strength of the honeycomb structure, and the 100% PLA samples were approximately 1.3 times the specific strength of the honeycomb structure. It is clear that the 100% infill has a measurably higher specific strength.

Another potential variable of the FDM printing process is the feed rate of
595 the print filament; a higher feed rate will clearly speed up the printing process, leading to quicker production times and lower costs. [20] consider the effect of this on the tensile strength of samples, investigating the impact of three feed rates: 20mm/s, 50mm/s and 80mm/s. The study also considers print orientation and layer height. In the upright build orientation, an increase in
600 feed rate results in a measurable drop in tensile strength of the samples across all layer heights. For the flat and on-edge samples, feed rate appears to have minimal impact on the tensile strength of the samples.

In addition to investigating the impact of PLA colour on the tensile strength of samples as discussed in Section 4.1, [38] also consider the effect of varying the
605 extruder temperature when using ‘RepRap’ type printers. Four printing temperatures are investigated: 190°C, 200°C, 210°C and 215°C. A large variation is apparent in the results but a general correlation of increasing yield strength with increasing extruder temperature is observed, however there is a slight dip in sample yield strength at a temperature of 200°C. Reasons for this observed
610 behaviour will be discussed in Section 5.6.

5. Discussion

5.1. Material selection

Overall, the studies considering the effect of material selection on tensile strength find that PLA, PC and PEEK all out-perform ABS. Various reasons
615 are discussed for this. In addition to higher tensile strength, [6] suggest that PC samples showed much lower coefficients of variation (COV), a measure of relative variability, than the ABS samples. The study points out that the printer used for manufacturing the PC samples was a professional grade printer, compared to the ‘hobby-grade’ printer used for the ABS samples; this could have affected
620 variability and quality of the produced samples.

The study by [14] utilise a range of ‘Rep-rap’ printers of a similar grade to compare ABS and PLA and demonstrate that PLA has a higher tensile strength. The failure surfaces of these samples are assessed and it is found that PLA specimens demonstrate superior inter-raster and inter-layer bonding, appearing more like a “homogeneous solid than a composition of individual extruded rasters”. This superior bonding will lead to improved tensile strength performance. This is further supported by the claim in this study that ‘Rep-Rap’ printed PLA samples can achieve comparable strength to injection moulded PLA parts (which are a homogeneous solid, without inter-raster or inter-layer bonds). ‘Rep-Rap’ ABS parts however, are generally weaker than injection moulded alternatives. The fact that ‘Rep-Rap’ printed PLA parts can achieve tensile strengths equivalent to injection moulded parts demonstrates the quality of the inter-raster and inter-layer bonding in parts printed with this material. The study also suggests there is significant variety in filament characteristics even for the same material classification and argues filament vendors should provide better data including composition and mechanical test data for the printing filament itself.

It is also suggested by [29] that inter-raster and inter-layer bonding may be the cause of different tensile strength results. In this study SEM (Scanning Electron Microscope) imaging is used to review fracture surfaces and again finds that in ABS samples the individual rasters can be clearly seen. However, in the stronger PEEK samples, the fracture surface appears to be one homogeneous block. Given the relatively new introduction of PEEK this study suggests that, in time, the printing parameters with this material can be further optimised leading to an even greater tensile strength improvement over ABS.

The investigation by [15] that considers including additives to create an ABS composite also utilises SEM to interpret the observed results. For those samples loaded with jute fibre and printed in the flat plane, the fractured samples were shown to have “multiple craters and voids”, which would clearly lead to a reduction in tensile strength. This is believed to be due to the decomposition of the jute fibre at 180°C, well below the extrusion temperature used in the printing process. This process of decomposition leads to by-products and gases creating the observed voids. ABS samples incorporating TiO₂ were shown to have the highest tensile strength and the study suggests the presence of TiO₂ limits the ability of the plastic macromolecules to slide over one another, which can be seen by the brittle fracture surface observed in the samples. Brenken et al. [8] also cite void formation, in addition to fibre damage during printing, as reasons for under-performing fibre reinforced composites. This review also highlights the importance of sufficient wetting of the composite fibres during the printing process to maximise the strength of continuous fibre composites.

Further demonstrating the variation within material classifications [38] show a significant variation between PLA samples printed with different colour filaments; natural PLA, with no added dye, has the highest tensile strength. X-ray powder diffraction (XRD) is utilised to understand the reasons for this variation. It is found that the variation in tensile strength is related to the crystallinity of the printed parts, which is dependent on filament colour; the specimens printed

using natural PLA have the lowest % crystallinity when analysed utilising XRD.

5.2. Raster orientation

There is a majority consensus amongst the studies considering ABS that the highest tensile strength is achieved with a 0° raster angle. This is due to the alignment of the tensile loading along the length of the raster (trans-raster strength) as opposed to across inter-raster bonds. [34] however does warn that, whilst achieving the highest tensile strength, samples printed with a 0° raster angle are more susceptible to variations in the strength of the mono-filament feedstock than samples printed with alternative raster directions.

Interestingly, [19] look at the relative strength of a range of different sized hour-glass ABS specimens, printed with consistent printing parameters. This work demonstrates that the dimensions of the specimen can affect what optimum printing parameters are required to achieve maximum UTS.

Although a variety of results are reported by [22], the highest tensile strength in the ABS samples is obtained with a raster angle of 60° . This higher raster angle results in shorter raster lengths in the samples and the paper suggests these shorter raster lengths reduce distortion in the samples, increasing their strength. Conversely, the paper also suggests that lower raster angles (e.g. 0°) result in tensile loading along the length of the raster which should improve strength, as suggested by many of the other publications.

Fewer studies are conducted looking at the effect of raster angle on PLA samples and there is reduced consensus with alteration to raster angle appearing to have less impact on sample tensile strength. This could be due to the improved inter-raster and inter-layer bonding achieved with PLA as discussed in Section 5.1. Interestingly [13] review the quality of the printed samples and observe that for the 0° samples a gap is apparent between the ‘shell’ and the main body of the specimen due to the construction of the raster roads. Gaps such as this will certainly weaken the structure, leading to lower tensile strength. In some cases, this gap led to the outer shell separating from the main body of the sample during tensile testing. This gap however, is not apparent in the 45° and 90° samples. This finding suggests the 0° raster angle is less well suited to the specific geometry of the tensile test samples but may not necessarily produce weaker products overall.

A further PLA study by [18] finds that 0° raster angle has the highest UTS followed by 45° then 90° . In agreement with many of the ABS studies, this paper cites the alignment of the tensile load along the raster roads as the predominant reason for the superior tensile performance with 0° rasters. This theory is also supported by [29], who demonstrate superior strength in PEEK printed with a 0° raster angle, and [4], who make the same conclusion for PC samples.

5.3. Print orientation

Although there is some variation in the results, most of the studies agree that samples printed in the upright orientation perform significantly worse in tensile testing than those printed flat or on-edge. [25] suggests that the noticeable

710 weakness in the upright samples occurs due to the predominant load being
 carried across the printed layers rather than along the length of the rasters;
 the links between adjacent layers are referred to as inter-layer fusion bonds by
 [20]. This inter-layer bonding between consecutive layers is much weaker than
 the trans-raster strength along the length of the rasters, and hence samples
 715 printed in the upright direction prove to be significantly weaker. This theory is
 supported by [20] who suggest the difference in UTS due to print orientation is
 attributable to the increased number of the weaker, inter-layer fusion bonds in
 the upright samples.

Interestingly, [6] observe very little variation in tensile strength with print
 720 orientation in ABS but significant variation with PC samples. This demon-
 strates that print orientation needs to be optimised for the selected printing
 material (as the strength of the inter-layer and inter-raster bonds will be strongly
 affected by printing material as well as print parameters).

Print direction will also effect printing times and hence production costs.
 725 This is addressed by [25] and [20] where the data shows both flat and on-edge
 samples printed to ASTM D638 dimensions are significantly quicker to print
 than upright samples (although print time is also affected by layer height). The
 consideration of print time provides further confirmation that upright printing
 should be avoided.

It is clear from most of the studies that FDM printed samples demonstrate
 730 significant anisotropy and some further studies have looked at techniques for re-
 ducing this behaviour. For example, [41] utilise ionizing radiation with copoly-
 mer blends to improve the mechanical performance of PLA. Through exposure
 to gamma rays post printing, inter-layer adhesion of the samples was improved
 735 via the introduction of crosslinks between polymer chains. This study demon-
 strates this technique can be used to improve the tensile strength of FDM sam-
 ples and reduce anisotropy. Another study by [37] also seeks to reduce the
 anisotropy of FDM printed samples by enhancing ABS with additives. Six
 polymer matrix and four polymer blends are investigated, and although it is
 740 shown that anisotropy can be reduced, this comes at the expense of an overall
 reduction in the UTS of the samples.

Further studies of this nature have the potential to both reduce anisotropy
 and improve the mechanical performance of FDM printed samples, and are an
 area of continued research.

745 5.4. Layer height

The effect of layer height on ABS printed samples is investigated by [22] who,
 in contrast to other papers find that a thicker layer height results in higher tensile
 strength. The authors discuss a range of reasons for the observed variations.
 A greater number of layers can result in a high temperature gradient at the
 750 base of the part which can improve strength by increasing the diffusion between
 adjacent rasters but it can also decrease strength as the temperature gradient
 can lead to sample distortion. They also suggest a higher number of layers
 increases the number of heating and cooling cycles the sample is subject to,
 which can result in the accumulation of residual stress within the sample. The

755 authors therefore suggest that increasing the individual layer height reduces the total number of layers required, which, due to the above reasons, increases the strength of the sample.

The opposite effect is observed in a study by [5], who also consider ABS. Here, the lower layer height results in higher sample UTS. To understand this behaviour, this study investigates the printed sample structures by using a Keyence VHX-600 digital microscope to quantify the air-gap to material ratio for samples printed with differing layer heights. The sample printed with a greater layer height, 0.4mm, had a 5.26% air-gap to material ratio compared to the 0.2mm layer sample, which had a 0.3% ratio. This reduced air-gap to material ratio for the samples with lower layer height results in more material to carry the tensile load and hence a higher UTS.

These results are further supported by [20] who find that for PLA samples printed in a flat or on-edge orientation a lower layer height results in a higher tensile strength. For samples printed in an upright orientation however, the lower layer height reduces the tensile strength. This is due to the previously discussed issue of inter-layer fusion between consecutive layers resulting in weaker links than trans-raster loading. In an upright sample, a reduction in layer height actually increases the number of weak inter-layer fusion bonds across which the tensile force is experienced, resulting in a reduction in overall tensile strength.

As discussed in Section 5.3, layer height will also affect printing time and therefore production costs. It is shown by [20] that the lower the layer height, the longer the printing time; reducing layer height from 0.24mm to 0.06mm can increase the print time by up to 300%. Despite the fact that reducing layer height can improve product mechanical properties, this must be balanced against the associated increase in print time and production costs. The optimal solution will therefore be very project and product dependant.

5.5. Air gap and raster width

The effect of varying the air gap and the sensitivity of this depending on raster angle selection is highlighted by [16] who find that a slightly negative air gap produces samples with the highest UTS. The negative air gap creates better bonding between adjacent raster roads and hence improves the UTS of the samples at all raster angles. The effect of increasing the air gap has an increasingly negative impact on 45° and 90° raster angles because, due to the tensile loading direction, the tensile strength of these samples is more reliant on inter-raster bonding. Increasing the air gap in this instance reduces the strength of the inter-raster bonding and hence reduces the overall UTS of the samples. In samples with a 0° raster angle the loading is predominantly trans-raster so although increasing the air gap does reduce the strength of the samples, the effect is not as severe as for samples with 45° and 90° raster angles.

The pattern of a higher observed UTS with smallest air gap is also observed in a study by [39] who find that a negative air gap consistently results in a higher sample UTS across a range of variables tested in ABS samples. As described above, the negative air gap essentially leads to better bonding between

consecutive raster roads in a given layer and there is more material to carry the tensile load for a given unit area; hence the UTS goes up. This paper also considers the effect of raster width, and demonstrates that optimum tensile strength is achieved when correctly selecting raster width and air gap to be complementary, achieving optimum bonding between consecutive raster roads. This paper does warn about ‘overfill’ flaws in samples occurring when a negative air gap is used with a thicker raster width, essentially resulting in a 12.5% overlap between raster roads. This ‘overfill’ can create flaws and an unpleasant surface appearance and is shown to slightly reduce the UTS of the samples investigated. The correct balance between air gap and raster width must be achieved to ensure minimal air gap and good bonding between consecutive raster roads without excessive material leading to instances of ‘overfill’.

5.6. Other variables

The effect of the infill pattern is investigated by [26] who consider a 100% infill density in comparison to a honeycomb structure. This study finds that the specific strength of the honeycomb structure is measurably less than that of the filled structure. The study concludes that despite making a more lightweight structure that will be quicker to print, the loss in strength when utilising an infill pattern should be considered.

Filament feed rate is found to have minimal impact on the tensile strength of PLA samples printed in the flat and on-edge orientations within the bounds tested (20-80 mm/s) by [20]. A higher feed rate can be selected in these instances to speed up the printing process. However, for samples printed in the upright direction, a higher speed rate can reduce the tensile strength of the samples and should be avoided. This could be due to the increased number of inter-layer bonds in the upright samples which may be weaker with a higher feed rate.

A general trend of increasing sample yield strength with extruder temperature is observed by [38] when using a ‘RepRap’ printer to print PLA samples. The study also considers the effect of extruder temperature on the crystalline structure of samples utilising XRD. The lowest % crystallinity was observed for the samples printed at 200°C and this also corresponds with the lowest yield strength of all the samples. This trend does not follow throughout the other results however, as crystallinity peaks at 210°C and then significantly drops off but tensile strength continues to increase. The study also suggests that a higher printing temperature may allow better inter-layer bonding to occur before the printing materials cool to the glass transition temperature. This improved inter-layer bonding will result in higher yield strengths.

5.7. Overall discussion

The benefit of altering various printing parameters to optimise component tensile strength is clear to see in the presented results (Section 4). It should be highlighted however, that these studies are based on idealised samples with simple geometry specifically developed for unidirectional tensile testing purposes. In reality, printed products will rarely have such simplicity and the loading and

hence stress distribution within them will be much more complex. The results presented must therefore be interpreted and optimised for any particular geometry. The use of FEA numerical models to identify the stress distribution and hence allow the user to select the optimum print parameters (such as print direction and raster angle) for that geometry should be considered.

The majority of the studies considered in this review are empirical studies presenting results from physical test campaigns. Whilst this satisfies the main objective of this paper, studies addressing the physical processes governing FDM printing provide further insight into the observed results, and highlight opportunities to use predictive tools and numerical models to predict printed component properties. This area of study is addressed by [8] who discuss several studies of interest.

For example, the tensile strength of printed components has been shown to be strongly dependant on the strength of the inter-raster and inter-layer bonds. Various physical processes govern the formation of these bonds and are considered in detail by [42, 43, 44, 45], with [16] developing filament and macro scale FE models to consider the effect of raster angle and air gap in ABS printed parts and comparing results to a physical test campaign. In addition to this, the heat transfer and solidification of the printed parts will also affect the tensile strength. Two early papers, [46] and [47], develop 1D and 2D models respectively of the thermal processes involved in FDM. Further studies have been conducted to develop the understanding of these processes including [48, 49, 50, 51, 52, 53] and [54].

The high temperatures involved in the printing process can also lead to residual stress accumulation and/or deformation in the produced part. Analytic solutions for simple geometries have been developed to predict the warpage of printed components by [48] and [55]. A 3D FEA model of the printing process is developed by [56] and is subsequently used to develop experimental investigations [57]. 3D simulations of composite printed parts are also presented by [58] and [59].

Despite this large body of work, investigating and modelling the physical processes involved in FDM additive manufacturing, the conclusion of the review paper by [8] is that many of the models are overly simplified, and do not fully describe the processes. It is suggested that future research should seek to develop further modelling tools to more accurately predict the printing outcomes and therefore create more certainty on printed product mechanical properties.

6. Conclusions

Additive manufacturing is a rapidly developing sector, with continual progress in printed product quality. With these developments the technology is transitioning from a prototype printing tool to a manufacturing method in its own right. FDM is one of the most common forms of 3D printing with many hobbyist as well as professional printers adopting this technology. With numerous printing variables available for each print run, having the knowledge to opti-

mise the printing process to achieve particular material properties is clearly advantageous.

This paper has reviewed a range of recent publications aiming to optimise the FDM printing process in order to improve the tensile strength of printed samples. Reviewing the range of methodologies applied by the different studies highlights the need for specific methodologies for the mechanical testing of additive manufactured components. This would allow for a more systematic approach across the sector. Any new methodology should permit test pieces of greater thickness to allow for investigation into the many internal structures possible with 3D printed products.

Although not all the studies concur on all printing variables, some key recommendations can be made to optimise the tensile strength of samples as detailed below.

1. **Material:** On average, PLA is shown to have 1.1 to 2 times the tensile strength of ABS. PC is shown to have 1.9 times the tensile strength of ABS, and PEEK is shown to have 2.1 times the strength of ABS, with a high potential for further improvement through printing optimisation. Additives to standard materials can both improve and reduce the tensile performance of FDM samples; adding TiO_2 to ABS was shown to improve tensile strength. Overall, continuous fibre reinforced composites show the highest potential for tensile strength improvement. Even the colour of PLA filament can effect tensile strength, with the strongest samples manufactured from natural PLA with no added dye.
2. **Raster angle:** Many studies considered the effect of raster angle on ABS samples with the majority concurring that a 0° raster angle, where the predominant load is carried along the length of the raster, resulted in the highest tensile strength. In some cases this achieved 2 times the tensile strength of samples with a raster angle of 90° . Fewer studies were conducted with PLA, concluding that either 0° or 45° achieved highest tensile strength, with 90° raster angles resulting in weaker samples. PC studies also varied in conclusion with one study clearly demonstrating a better tensile performance for 0° raster angle and another study demonstrating marginally better tensile strength performance with $\pm 45^\circ$ raster angle.
3. **Print orientation:** Generally, printing in the upright orientation should be avoided if tensile strength is a priority. Printing in the flat or on-edge orientation achieves better tensile performance for ABS, PC and PLA, often achieving twice the tensile strength of up-right printed samples. Minimal variation is observed between the strength of flat and on-edge printed samples.
4. **Air gap/raster width:** Air gap and raster width should be optimised together, to ensure high quality inter-raster bonding without ‘overfill’. Consideration should be given to selecting a negative air gap to achieve this.

- 930 5. **Layer height:** For flat and on-edge orientations, layer height should be minimised in order to achieve maximum tensile strength. This improves the strength for both ABS and PLA samples considered, with one PLA study demonstrating a 24.5% tensile strength improvement when reducing layer height from 0.4mm to 0.2mm. Reduced layer height increases print time, so the improvement in tensile strength should be balanced against the increased manufacturing time (which leads to increased product costs). 935
6. **Other variables:** The following variables have been considered in this paper but need more investigation.
- (a) Infill: Numerous infill options are available, and the choice of infill should be selected to balance print time and print materials against the achieved product tensile strength. Clearly 100% infill will result in higher tensile strength, and one study demonstrated that it also showed highest specific strength. Further work is required on the numerous options available to optimise infill patterns and to strike the desired balance between printing time and materials used Vs. product tensile strength. 940 945
 - (b) Printing temperature: Although, only considered in one study, an increase in extruder temperature was shown to improve tensile strength performance due to improved inter-raster and inter-layer bonding. Further research on this topic is required.
 - 950 (c) Feed rate: The feed rate of the printing filament is considered in one study and is found to have limited effect on flat or on-edge samples though some effect is observed in upright samples. The feed rate should therefore be optimised to minimise printing time, rather than optimise material properties.

955 In summary, there are numerous printing parameters available when utilising AM technology. The conclusions presented in this paper can act as a robust and pragmatic reference point for users seeking to optimise their FDM printing processes regarding product tensile strength.

960 Research and development of new materials, different post processing techniques and alternative printing parameters will continue in this fast moving technology field. The development of numerical modelling packages to improve the prediction of material properties for these products is required, and is a key challenge for the sector given the fast pace of technology development. Undoubtedly, the mechanical properties of FDM printed components will continue to improve, making the use of this technology as a large scale production technique increasingly plausible. 965

7. Acknowledgements

This work was funded through the European Union under the European Regional Development Funding (ERDF) Marneir, Grant/Award Number: 05R16P00381.

970 The work was commissioned by 3D Kernow in order to optimise their printing
processes to better serve the additive manufacturing requirements of the marine
sector in the Cornwall and Isles of Scilly region.

References

- 975 [1] Grand View Research, Market research report: 3D Printing (3DP) market
analysis by printer type (desktop, industrial), by technology, by software,
by application, by vertical, by region, and segment forecasts, 2018-2025
(2017).
URL [https://www.grandviewresearch.com/industry-analysis/
3d-printing-industry-analysis](https://www.grandviewresearch.com/industry-analysis/3d-printing-industry-analysis)
- 980 [2] B. Berman, 3-D printing: The new industrial revolution, *Business horizons*
55 (2) (2012) 155–162. doi:10.1016/j.bushor.2011.11.003.
- [3] C. Moreau, The state of 3D printing (2017).
URL [https://www.sculpteo.com/media/ebook/State%20of%203DP%
202017_1.pdf](https://www.sculpteo.com/media/ebook/State%20of%203DP%202017_1.pdf)
- 985 [4] N. Hill, M. Haghi, Deposition direction-dependent failure criteria for fused
deposition modeling polycarbonate, *Rapid Prototyping Journal* 20 (3)
(2014) 221–227. doi:10.1108/RPJ-04-2013-0039.
- [5] B. Rankouhi, S. Javadpour, F. Delfanian, T. Letcher, Failure analysis and
mechanical characterization of 3D printed ABS with respect to layer thick-
ness and orientation, *Journal of Failure Analysis and Prevention* 16 (3)
990 (2016) 467–481. doi:10.1007/s11668-016-0113-2.
- [6] J. T. Cantrell, S. Rohde, D. Damiani, R. Gurnani, L. DiSandro, J. An-
ton, A. Young, A. Jerez, D. Steinbach, C. Kroese, Experimental charac-
terization of the mechanical properties of 3D-printed ABS and polycar-
bonate parts, *Rapid Prototyping Journal* 23 (4) (2017) 811–824. doi:
995 10.1108/RPJ-03-2016-0042.
- [7] J. R. C. Dizon, A. H. Espera, Q. Chen, R. C. Advincula, Mechanical char-
acterization of 3D-Printed polymers, *Additive Manufacturing* 20 (2017)
44–67. doi:10.1016/j.addma.2017.12.002.
- 1000 [8] B. Brenken, E. Barocio, A. Favalaro, V. Kunc, R. B. Pipes, Fused filament
fabrication of fiber-reinforced polymers: A review, *Additive Manufacturing*
21 (2018) 1–16. doi:10.1016/j.addma.2018.01.002.
- [9] R. Jones, P. Haufe, E. Sells, P. Irvanvi, V. Olliver, C. Palmer, A. Bowyer,
RepRap - the replicating rapid prototyper, *Robotica* 29 (1) (2011) 177–191.
1005 doi:10.1017/S026357471000069X.

- [10] DNV GL, Additive manufacturing - qualification and certification process for materials and components (2017).
URL <https://rules.dnvgl.com/docs/pdf/DNVGL/CG/2017-11/DNVGL-CG-0197.pdf>
- 1010 [11] ASTM, ASTM D638-14 Standard test method for tensile properties of plastics, ASTM International (2014).
- [12] BSI, BS EN ISO 527-2:1996. Plastics - determination of tensile properties. part 2: Test conditions for moulding and extrusion plastics, BSI Group (1996).
- 1015 [13] T. Letcher, M. Waytashek, Material property testing of 3D-printed specimen in PLA on an entry-level 3D printer, in: ASME 2014 International Mechanical Engineering Congress and Exposition, American Society of Mechanical Engineers, 2014. doi:10.1115/IMECE2014-39379.
- 1020 [14] B. Tymrak, M. Kreiger, J. M. Pearce, Mechanical properties of components fabricated with open-source 3-D printers under realistic environmental conditions, *Materials & Design* 58 (2014) 242–246. doi:10.1016/j.matdes.2014.02.038.
- 1025 [15] A. R. Torrado Perez, D. A. Roberson, R. B. Wicker, Fracture surface analysis of 3D-printed tensile specimens of novel ABS-based materials, *Journal of Failure Analysis and Prevention* 14 (3) (2014) 343–353. doi:10.1007/s11668-014-9803-9.
- 1030 [16] H. Rezayat, W. Zhou, A. Siriruk, D. Penumadu, S. Babu, Structure-mechanical property relationship in fused deposition modelling, *Materials Science and Technology* 31 (8) (2015) 895–903. doi:10.1179/1743284715Y.0000000010.
- 1035 [17] T. Letcher, B. Rankouhi, S. Javadpour, Experimental study of mechanical properties of additively manufactured ABS plastic as a function of layer parameters, in: ASME 2015 International Mechanical Engineering Congress and Exposition, American Society of Mechanical Engineers, 2015, pp. V02AT02A018–V02AT02A018. doi:10.1115/IMECE2015-52634.
- [18] M. F. Afrose, S. Masood, P. Iovenitti, M. Nikzad, I. Sbarski, Effects of part build orientations on fatigue behaviour of FDM-processed PLA material, *Progress in Additive Manufacturing* 1 (1-2) (2016) 21–28. doi:10.1007/s40964-015-0002-3.
- 1040 [19] A. R. Torrado Perez, D. A. Roberson, Failure analysis and anisotropy evaluation of 3D-printed tensile test specimens of different geometries and print raster patterns, *Journal of Failure Analysis and Prevention* 16 (1) (2016) 154–164. doi:10.1007/s11668-016-0067-4.

- 1045 [20] J. Chacn, M. Caminero, E. Garca-Plaza, P. Nez, Additive manufacturing of PLA structures using fused deposition modelling: effect of process parameters on mechanical properties and their optimal selection, *Materials & Design* 124 (2017) 143–157. doi:10.1016/j.matdes.2017.03.065.
- [21] J. Kotlinski, Mechanical properties of commercial rapid prototyping materials, *Rapid Prototyping Journal* 20 (6) (2014) 499–510. doi:10.1108/RPJ-06-2012-0052.
- 1050 [22] A. K. Sood, R. K. Ohdar, S. S. Mahapatra, Parametric appraisal of mechanical property of fused deposition modelling processed parts, *Materials & Design* 31 (1) (2010) 287–295. doi:10.1016/j.matdes.2009.06.016.
- [23] D. Drummer, S. Cifuentes-Cuellar, D. Rietzel, Suitability of PLA/TCP for fused deposition modeling, *Rapid Prototyping Journal* 18 (6) (2012) 500–507. doi:10.1108/13552541211272045.
- 1055 [24] J. Lee, A. Huang, Fatigue analysis of FDM materials, *Rapid Prototyping Journal* 19 (4) (2013) 291–299. doi:10.1108/13552541311323290.
- [25] I. Durgun, R. Ertan, Experimental investigation of FDM process for improvement of mechanical properties and production cost, *Rapid Prototyping Journal* 20 (3) (2014) 228–235. doi:10.1108/RPJ-10-2012-0091.
- 1060 [26] E. Ebel, T. Sinnemann, Fabrication of FDM 3D objects with ABS and PLA and determination of their mechanical properties, *RTejournal* 2014 (1).
 1065 URL http://www.rtejournal.de/ausgabe11/3872/view?set_language=de
- [27] K. Szykiedans, W. Credo, Mechanical properties of FDM and SLA low-cost 3D prints, *Procedia Engineering* 136 (2016) 257–262. doi:10.1016/j.proeng.2016.01.207.
- 1070 [28] BSI, BS EN ISO 527-3:1996 Plastics. Determination of tensile properties. Test conditions for films and sheets., BSI Group.
- [29] W. Wu, P. Geng, G. Li, D. Zhao, H. Zhang, J. Zhao, Influence of layer thickness and raster angle on the mechanical properties of 3D-printed PEEK and a comparative mechanical study between PEEK and ABS, *Materials* 8 (9) (2015) 5834–5846. doi:10.3390/ma8095271.
- 1075 [30] Y. Song, Y. Li, W. Song, K. Yee, K.-Y. Lee, V. Tagarielli, Measurements of the mechanical response of unidirectional 3D-printed PLA, *Materials & Design* 123 (2017) 154–164. doi:10.1016/j.matdes.2017.03.051.
- [31] S.-H. Ahn, M. Montero, D. Odell, S. Roundy, P. K. Wright, Anisotropic material properties of fused deposition modeling ABS, *Rapid Prototyping Journal* 8 (4) (2002) 248–257. doi:10.1108/13552540210441166.
- 1080

- [32] BSI, BS EN ISO 527-5:1997. Plastics - determination of tensile properties. part 5: Test conditions for uni-directional fibre-reinforced plastic composites, BSI Group (2009).
- 1085 [33] ASTM, ASTM D3039-17 Standard test method for tensile properties of polymer matrix composite materials, ASTM International (2017).
- [34] C. Ziemian, M. Sharma, S. Ziemian, Anisotropic mechanical properties of ABS parts fabricated by fused deposition modelling (2012).
URL <http://cdn.intechopen.com/pdfs/35261.pdf>
- 1090 [35] Intertek, Tensile properties. ASTM D638 Vs. ASTM D3039, Report, Interek Plastics Technology Laboratories (2018).
URL www.intertek.com/polymers/tensile-properties-testing/brochure/
- 1095 [36] C. Wendt, M. Batista, E. Moreno, A. Valerga, S. Fernandez-Vidal, O. Droste, M. Marcos, Preliminary design and analysis of tensile test samples developed by additive manufacturing, *Procedia engineering* 132 (2015) 132–139. doi:10.1016/j.proeng.2015.12.489.
- [37] A. R. Torrado Perez, C. M. Shemelya, J. D. English, Y. Lin, R. B. Wicker, D. A. Roberson, Characterizing the effect of additives to ABS on the mechanical property anisotropy of specimens fabricated by material extrusion 3D printing, *Additive Manufacturing* 6 (2015) 16–29. doi:<https://doi.org/10.1016/j.addma.2015.02.001>.
- 1100 [38] B. Wittbrodt, J. M. Pearce, The effects of pla color on material properties of 3-D printed components, *Additive Manufacturing* 8 (2015) 110–116. doi:10.1016/j.addma.2015.09.006.
- 1105 [39] F. Rayegani, G. C. Onwubolu, Fused deposition modelling (FDM) process parameter prediction and optimization using group method for data handling (GMDH) and differential evolution (DE), *The International Journal of Advanced Manufacturing Technology* 73 (1-4) (2014) 509–519. doi:10.1007/s00170-014-5835-2.
- 1110 [40] Ultimaker, Ultimaker manual: Infill, Online (2018).
URL <https://ultimaker.com/en/resources/20416-infill>
- [41] S. Shaffer, K. Yang, J. Vargas, M. A. Di Prima, W. Voit, On reducing anisotropy in 3D printed polymers via ionizing radiation, *Polymer* 55 (23) (2014) 5969–5979. doi:10.1016/j.polymer.2014.07.054.
- 1115 [42] L. Li, Q. Sun, C. Bellehumeur, P. Gu, Investigation of bond formation in FDM process, *Solid Freeform Fabrication Proceedings*, (2002) 400407.
URL <http://sffsymposium.engr.utexas.edu/Manuscripts/2002/2002-45-Li.pdf>

- [43] C. Bellehumeur, L. Li, Q. Sun, P. Gu, Modeling of bond formation between polymer filaments in the fused deposition modeling process, *Journal of Manufacturing Processes* 6 (2) (2004) 170–178. doi:10.1016/S1526-6125(04)70071-7.
- [44] Q. Sun, G. Rizvi, C. Bellehumeur, P. Gu, Effect of processing conditions on the bonding quality of FDM polymer filaments, *Rapid Prototyping Journal* 14 (2) (2008) 72–80. doi:10.1108/13552540810862028.
- [45] P. K. Gurralla, S. P. Regalla, Part strength evolution with bonding between filaments in fused deposition modelling: This paper studies how coalescence of filaments contributes to the strength of final FDM part, *Virtual and Physical Prototyping* 9 (3) (2014) 141–149. doi:10.1080/17452759.2014.913400.
- [46] M. A. Yardimci, S. Geri, Conceptual framework for the thermal process modelling of fused deposition, *Rapid Prototyping Journal* 2 (2) (1996) 26–31. doi:10.1108/13552549610128206.
- [47] M. Yardimci, T. Hattori, S. I. Guceri, S. C. Danforth, Thermal analysis of fused deposition, in: *Solid Freeform Fabrication (SFF) Symposium*, 1996. URL <https://pdfs.semanticscholar.org/04e6/6000ff7b361e89b7928d54b4b194df9c54e0.pdf>
- [48] T.-M. Wang, J.-T. Xi, Y. Jin, A model research for prototype warp deformation in the FDM process, *The International Journal of Advanced Manufacturing Technology* 33 (11-12) (2007) 1087–1096. doi:10.1007/s00170-006-0878-7.
- [49] S. F. Costa, F. M. Duarte, J. A. Covas, Towards modelling of free form extrusion: analytical solution of transient heat transfer, *International Journal of Material Forming* 1 (1) (2008) 703–706. doi:10.1007/s12289-008-0312-9.
- [50] S. Costa, F. Duarte, J. A. Covas, Using MATLAB to compute heat transfer in free form extrusion, *InTech*, 2011. URL <https://core.ac.uk/download/pdf/55745930.pdf#page=465>
- [51] S. Costa, F. Duarte, J. Covas, Thermal conditions affecting heat transfer in FDM/FFE: a contribution towards the numerical modelling of the process, *Virtual and Physical Prototyping* 10 (1) (2015) 35–46. doi:10.1080/17452759.2014.984042.
- [52] B. Brenken, A. Favaloro, E. Barocio, N. DeNardo, R. Pipes, Development of a model to predict temperature history and crystallization behavior of 3D printed parts made from fiber-reinforced thermoplastic polymers, in: *SAMPE conference*, Long Beach, CA, 2016. URL [http://refhub.elsevier.com/S2214-8604\(17\)30447-5/sbref0400](http://refhub.elsevier.com/S2214-8604(17)30447-5/sbref0400)

- 1160 [53] Y. Zhou, T. Nyberg, G. Xiong, D. Liu, Temperature analysis in the fused
deposition modeling process, in: Information Science and Control Engi-
neering (ICISCE), 2016 3rd International Conference on, IEEE, 2016, pp.
678–682. doi:10.1109/ICISCE.2016.150.
- 1165 [54] K. Pooladvand, C. Furlong, Thermo-mechanical investigation of fused
deposition modeling by computational and experimental methods, Me-
chanics of Composite and multi-functional materials 7 (2017) 45–54.
URL [https://link.springer.com/chapter/10.1007/
978-3-319-41766-0_6](https://link.springer.com/chapter/10.1007/978-3-319-41766-0_6)
- 1170 [55] L. Xinhua, L. Shengpeng, L. Zhou, Z. Xianhua, C. Xiaohu, W. Zhongbin,
An investigation on distortion of PLA thin-plate part in the FDM process,
The International Journal of Advanced Manufacturing Technology 79 (5-8)
(2015) 1117–1126. doi:10.1007/s00170-015-6893-9.
- 1175 [56] Y. Zhang, Y. K. Chou, 3D FEA simulations of fused deposition modeling
process, in: ASME 2006 International Manufacturing Science and Engi-
neering Conference, American Society of Mechanical Engineers, 2006, pp.
1121–1128. doi:10.1115/MSEC2006-21132.
- 1180 [57] Y. Zhang, K. Chou, A parametric study of part distortions in fused deposi-
tion modelling using three-dimensional finite element analysis, Proceedings
of the Institution of Mechanical Engineers, Part B: Journal of Engineering
Manufacture 222 (8) (2008) 959–968. doi:10.1243/09544054JEM990.
- 1185 [58] M. Talagani, S. DorMohammadi, R. Dutton, C. Godines, H. Baid, F. Abdi,
V. Kunc, B. Compton, S. Simunovic, C. Duty, et al., Numerical simulation
of big area additive manufacturing (3D printing) of a full size car, SAMPE
Journal 51 (4) (2015) 27–36.
URL <https://tinyurl.com/y6ughkrn>
- 1190 [59] A. J. Favaloro, B. Brenken, E. Barocio, R. B. Pipes, Simulation of
polymeric composites additive manufacturing using Abaqus, Science in
the Age of Experience, Chicago, IL (2017).
URL [http://refhub.elsevier.com/s2214-8604\(17\)30447-5/
sbref0455](http://refhub.elsevier.com/s2214-8604(17)30447-5/sbref0455)